## Block Copolymer Additives for Toughening 3D Printable Epoxy Resin

Ri Chen<sup>a‡</sup>, Jizhe Cai<sup>b‡</sup>, Kyle C.H. Chin<sup>d</sup>, Sheng Wang<sup>a</sup>, A J Boydston<sup>a,c,d</sup>, Ramathasan Thevamaran<sup>b\*</sup>, Padma Gopalan<sup>a,c,d,\*</sup>

‡Equally contributed authors

Key Words: Epoxy resin, 3D printing, block copolymer, synergistic strength and toughness

#### **Abstract**

We explore the potential for using a brush-coil triblock copolymer to enhance the mechanical properties of epoxy resin for 3D printing applications. Epoxy resins are widely used in structural material and adhesive and have great potential for 3D printing. However, the highly brittle nature of epoxy resins requires the use of large concentrations of toughening agents that pose significant challenges in meeting rheological requirements of 3D printing. We report a reactive brush-coil block copolymer with three distinct blocks that can phase separate, and chemically crosslink with the base epoxy resin to form spherical aggregates. Detailed scanning electron microscopy imaging shows that these aggregates can arrest and deflect cracks during propagation and can synergistically strengthen ( $\sim 1.5\times$ ) and toughen ( $\sim 2\times$ ) the epoxy resin with even 1wt % of the BCP additive to the base resin. Importantly both the modulus and the glass transition temperatures are preserved. Direct ink writing (DIW) and Digital light processing (DLP) 3D printing of the modified resins also shows the same strengthening and toughening effects seen in mold cast samples, demonstrating its compatibility with 3D printing processes. These findings suggest that brush-coil triblock copolymers additives at very low concentrations can synergistically improve the mechanical properties of epoxy resin for 3D printed parts.

*Keywords:* 3D printing, epoxy resins, brush-coil copolymers

#### 1. Introduction

Research in 3D printing (also known as additive manufacturing) has accelerated over the last decade due to its ability to custom design complex shapes. Potential applications of these custom

<sup>&</sup>lt;sup>a</sup> Department of Materials Science and Engineering, University of Wisconsin-Madison, Madison, Wisconsin 53706, United States

<sup>&</sup>lt;sup>b</sup> Department of Mechanical Engineering, University of Wisconsin-Madison, Madison, Wisconsin 53706, United States

<sup>&</sup>lt;sup>c</sup> Department of Chemistry, University of Wisconsin-Madison, Wisconsin 53706, United States

<sup>&</sup>lt;sup>d</sup> Department of Chemical and Biological Engineering, University of Wisconsin-Madison, Wisconsin 53706, United States

<sup>\*</sup>Corresponding authors email: thevamaran@wisc.edu (RT), pgopalan@wisc.edu (PG)

printed components are already showing great potential in soft-robots [1,2] microfluidics [3] and tissue engineering [4]. Based on the nature of the process, printing can be broadly categorized into those that undergo a physical change such as melting or softening and those that require a chemical change such as chemical crosslinking [5]. The methods based on chemical crosslinking are particularly attractive as the process can be expanded to thermosetting resins that are typically hard to print [6,7]. Prime among them is epoxy resin chemistry.

Epoxy resins have high modulus, good thermomechanical properties, and good chemical resistance leading to a wide range of applications in composites, adhesives and coatings [8]. However, the highly crosslinked nature of the resin makes them brittle and unsuitable for many applications without further modifications. Some of the common approaches used to toughen commercial epoxy resins add soft, rubbery fillers in the form of liquid rubber or rubber micro spheres [9]. The resulting soft spherical aggregates in the epoxy resin improve the toughness of the resin by arresting and deflecting crack propagation [8]. As a trade-off, increase in material toughness is often accompanied by the inevitable decrease of modulus, strength, and thermal properties such as glass transition temperature (15) 10 of the matrix polymer. These properties are closely tied to lack of interfacial adhesion of the additives to the matrix, which is well documented in multiphase material formulations [11]. In many of these studies the added rubber particles are dispersed in the epoxy but do not have significant adhesion to the base resin, thereby leading to deterioration of mechanical properties including the toughness. From a morphological perspective, both reactive and non-reactive block copolymer additives where one block is compatible/reactive with base epoxy resin, and the other is often rubbery incompatible block, have been studied. In most of these studies the base epoxy resin is aromatic diglycidyl ether of bisphenol A (DGEBA) based, and the block copolymer (BCP) additive is a linear di- or triblock, where under high BCP concentrations self-assembled structures [10,12-14] are observed. Often the choice of the rubbery blocks in these BCPs includes known elastomers such as poly(butyl acrylates), poly (butadiene), or poly(butadiene-acrylonitrile), blocks, but the coil blocks vary widely to be compatible with epoxy resin, such as PEO, PMMA, PS or polycaprolactone. For example, addition of 5-20 wt% of a non-reactive triblock copolymer poly(methyl methacrylate)-b-poly(butyl acrylate)-b-poly(methyl methacrylate) (MAM) to a Bisphenol A epoxy resin (E51) resulted in increased toughness but a decrease in tensile strength[15]. A reactive version of the same triblock resulted in further improvements in the toughness, but the strength and modulus values still decreased[16]. A recent report used just 1 wt% of a reactive core-shell bottlebrush copolymer with a rubbery block of PBA as core and an epoxy reactive block of polyglycidyl methacrylate (PGMA) as the shell, that resulted in increase in toughness while maintaining the elastic modulus, but the yield strength decreased by 10%[17]. There are numerous other studies that measure fracture toughness of a BCP/epoxy blend, but do not report the tensile strength or the modulus.[18]

Using these toughened resins in 3D printing poses other challenges, as the high BCP concentrations adversely affects the rheological properties by increasing the viscosity of the uncured resin [19,20]. The required viscosity for digital light processing (DLP) printing is quite low (<10 Pa·s)[20], whereas for methods such as direct ink writing (DIW) is relatively high (0.01-100 Pa·s at ~0.1 s<sup>-1</sup>) with an added requirement of shear thinning behavior for extrudability, and yield stress characteristics for retention of shape upon extrusion. [7]. In addition, for thermoset resins, the cure kinetics during these processes is also critically important

to have well defined printed parts. It is well known that polymer architectures have a profound influence on the rheological and self-assembly behavior [21]. Among them, bottlebrush copolymers have low viscosity in melt and in solution due to low interchain entanglements [22], and can self-assemble more easily due to favorable kinetics from low entanglements [23]. Both viscosity and morphology are important when using these BCPs as additives in 3D printing.

Simplification of the formulation with the least amount of additives can offer a generalizable resin platform, reduce cost to manufacture, and minimize processing variables that must be considered. In this work we explore an alternative BCP architecture that requires at most 1 wt% BCP concentration, hence largely preserving the rheological properties of the base resin. This gives flexibility to precure the resin to use in either DIW or DLP, if the cure kinetics can be accelerated. We demonstrate the design of a brush-coil BCP that can synergistically strengthen and toughen a commonly used cycloaliphatic epoxy base resin with low BCP concentration and is compatible with 3D printing (Figure 1). A soft, epoxy-phobic poly[monomethacryloxypropyl terminated polydimethylsiloxane (MAPDMS)] (PMAPDMS) block is selected for the coreforming brush block. For the epoxy-philic coil block, polystyrene (PS) chain is selected for its solubility in the resin. The flexible coil nature of the second block also allows for the formation of high curvature spherical aggregates [24,25]. A short, crosslinkable poly(glycidyl methacrylate) (PGMA) block is attached to the PS chain end to improve the interfacial adhesion by crosslinking with the base epoxy resin. We study the effect of increased BCP concentrations from 1-10 wt% in the base 3,4-epoxycyclohexylmethyl-3',4'-epoxycyclohexane carboxylate (ECC) resin, on its rheological, crosslinking, morphological, and mechanical properties. We demonstrate that with just 1 wt% BCP concentration, ~1.5 times improvement in strength and ~2 times improvement in toughness is achievable and more importantly we demonstrate the DIW from these modified resins. We further show that these BCPs can be incorporated into an ECC/acrylate blend and used for DLP process, with similar improvements in mechanical properties.

#### 2. Results and Discussion

## 2.1. Design and synthesis of bottlebrush

The brush-coil BCPs were synthesized via three sequential reversible addition fragmentation (RAFT) polymerization of monomethacryloxypropyl terminated polydimethylsiloxane (MAPDMS), styrene (S) and glycidyl methacrylate (GMA). The chain-end RAFT chain transfer agent (CTA) was substituted with a proton to avoid side reactions (see Supplementary Information for synthetic procedure and characterizations). The PMAPDMS provides the rubbery ( $T_g = -120\,^{\circ}\text{C}$ ) [26] block, and the brush architecture as the PDMS chains are grafted on to the polymerizable methacrylate backbone. The bottle brush architecture offers two advantages: 1) lower viscosity compared to its linear counterpart, and 2) elastomeric characteristic at lower weight % loading. The other two blocks composed of PS and PGMA. The PS chain is the epoxyphilic corona that also provides the glassy ( $T_g = 100\,^{\circ}\text{C}$ ) [27] component to retain mechanical properties. The  $T_g$  of the microphase segregated PS in epoxy resin is known to be lower than a bulk sample [28]. The terminal PGMA units provide the critical covalent anchoring to the epoxy base resin. To study the effect of composition of the BCP additive on the toughness of the base epoxy resin, three different PS block lengths were synthesized. To

understand the role of each block, three additional control samples with one of the three blocks missing were also synthesized (Figure 2, Table 1).

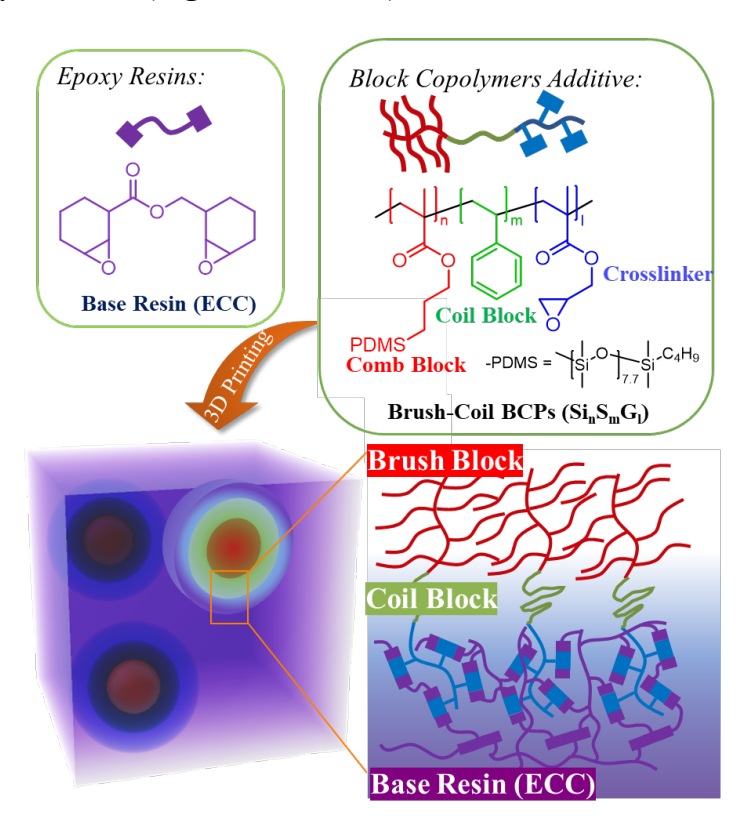


Figure 1: Structure of base resin, the custom designed brush-coil BCPs and the and the schematic of the expected morphology in the blend is depicted.

The thermal properties of the BCP additives were studied by DSC (**Figure 3**). In the first heating cycle, distinct  $T_g$ s corresponding to PGMA ( $T_g = 70$  °C [29]) and PS ( $T_g = 100$  °C), as well as an exothermic peak (140.5 °C) corresponding to the crosslinking of PGMA was observed. This indicates that most likely the PS and PMAPDMS are phase segregating and PGMA undergoes effective self- crosslinking. The crosslinking of PGMA was further confirmed by the disappearance of the  $T_g$  peak for PGMA in the second heating cycle. For  $Si_{11}S_{24}G_6$ , the thermal transitions were difficult to observe likely due to the short PS segment leading to disordered morphology. For control BCPs (**Figure S7**) $Si_8S_{61}$  and  $S_{25}G_1$ , single  $T_g$  for PS was detected. However, the  $T_g$  for PGMA was not observed likely due to short PGMA segment.

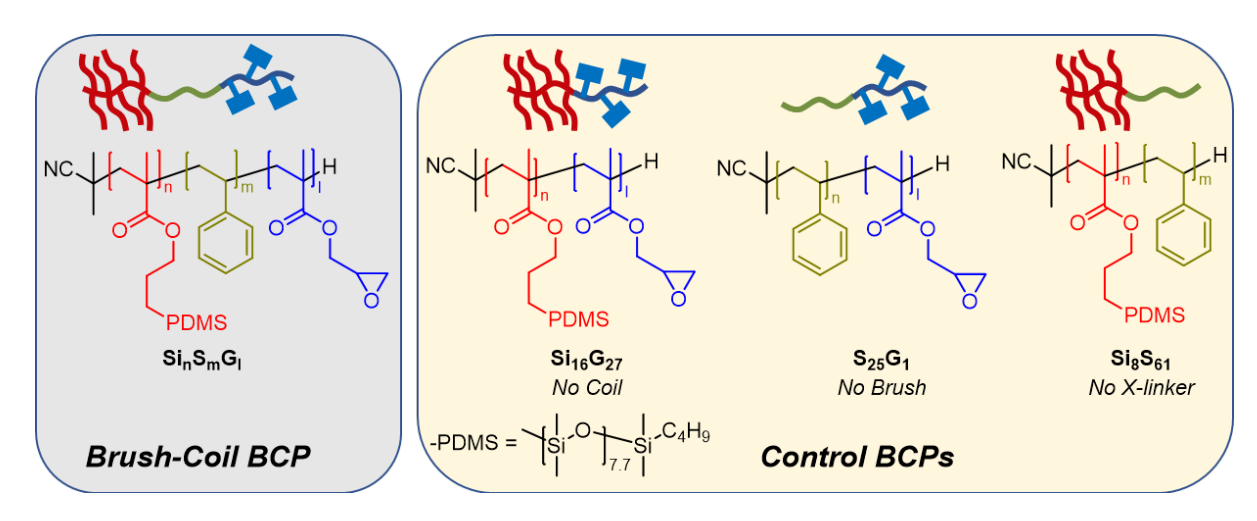


Figure 2: Structures of the brush-coil BCPs and controls studied.

Table 1: Composition of the Controls (in yellow) and the brush-coil BCPs (grey)

Sample name <sup>a)</sup>	$M_n[g/mol]^{b)}$	$f_{st}[\%]^{a)}$	Appearance
$Si_{16}G_{27}$	5764	0	Colorless, viscous liquid
$S_{25}G_1$	6312	0.93	White, solid powder
Si <sub>8</sub> S <sub>61</sub>	10954	0.55	White, solid powder
$Si_{11}S_{24}G_6$	7638	0.19	White, viscous liquid
$Si_{11}S_{80}G_{12}$	7308	0.45	White, rubbery solid
$Si_{11}S_{149}G_5$	9966	0.58	White, solid powder

<sup>&</sup>lt;sup>a)</sup> S stands for Styrene, G for GMA and Si for PMAPDMS. The subscript in the sample name corresponds to the degree of polymerization of each monomer in the final copolymer as determined by 1H NMR. <sup>b)</sup>  $M_n$  determined by GPC.

## 2.2. Block copolymer toughened resin curing

To test if these BCP additives will toughen the base resin, we first examined their solubility in the resin (**Figure 4**). We chose the cycloaliphatic resin, 3,4-epoxycyclohexylmethyl-3',4'-epoxycyclohexane carboxylate (ECC) as our base resin due to its widespread application in 3D printing [30]. The BCP (1 wt%) was dissolved in 2 mL of dichloromethane (DCM) and then mixed with ECC resin and dried under air flow with stirring. Upon drying, the control sample, without a PS block ( $Si_{16}G_{27}$ ), crashes out of the solution due to insolubility in the base resin, hence the epoxyphilic block is critical for its compatibility with ECC. Uniform dispersion was achieved with the BCPs with PS content equal or higher than in  $Si_{11}S_{80}G_{12}$  resulting in a clear solution. Turbidity test (**Figure S8**) also confirms this observation.

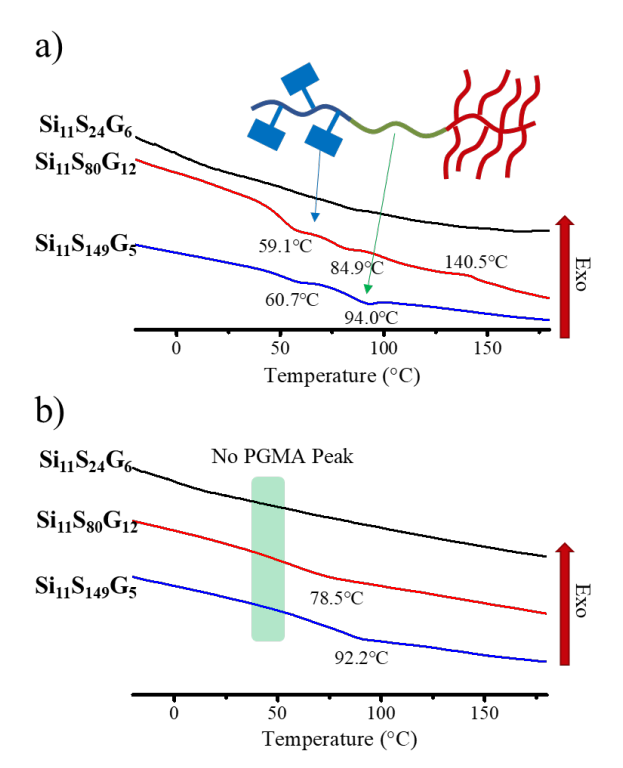


Figure 3: Differential scanning calorimetry (DSC) measurement of BCPs a) first heating cycle and b) second heating cycle. Exothermic points up.

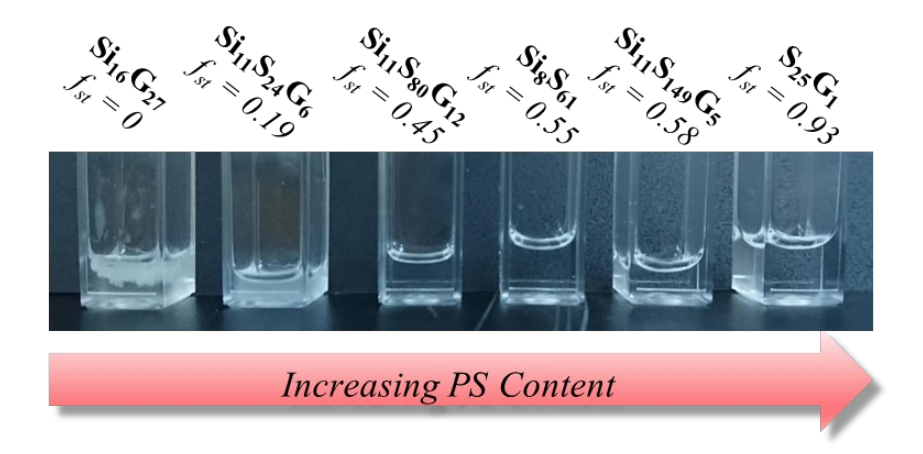


Figure 4: The solution turbidity indicates the improved solubility of BCPs (1 wt%) with increasing polystyrene content in the base ECC resin.

Mold-cast dog-bone samples were prepared from these blends to evaluate the mechanical properties in uniaxial tension (**Figure 5**). We first tested the control BCPs without core-forming PAPDMS block ( $S_{25}G_1$ ) or crosslinking PGMA block ( $S_{18}S_{61}$ ) and one brush-coil BCP ( $S_{111}S_{80}G_{12}$ ) against pure ECC resin. The ECC resin was mixed with a photoacid generator (triarylsulfonium hexafluoroantimonate salts, TAS) to initiate crosslinking and cured under UV light. These conditions are comparable to those in the actual 3D printing (See Supplementary Information for experimental details). We observed over 1.7 times increase in the toughness in  $S_{111}S_{80}G_{12}$  blends and an over 44% increase in the failure strength compared to the base ECC

resin. For the control  $S_{25}G_1$  blends, no further toughening compared to ECC resin was observed, as it does not contain the core forming PMAPDMS block. When the BCP additive is not crosslinked to the base resin, for example with the control blend of  $Si_8S_{61}$  with ECC, a smaller  $(0.44\times)$  enhancement in toughness was observed. Hence the presence of low  $T_g$  elastomeric PMAPDMS as well as covalent crosslinking of the additive with ECC via GMA units are important to enhance the toughness. Importantly, in all the BCP/ECC blends we did not observe a statistically significant decrease in the modulus. In fact, the  $T_g$  of the crosslinked blends measured by DSC (137 °C and 143 °C) show the least changes compared to the base resin (140 °C) (Figure 5(d)), hence the thermal characteristics are largely preserved.

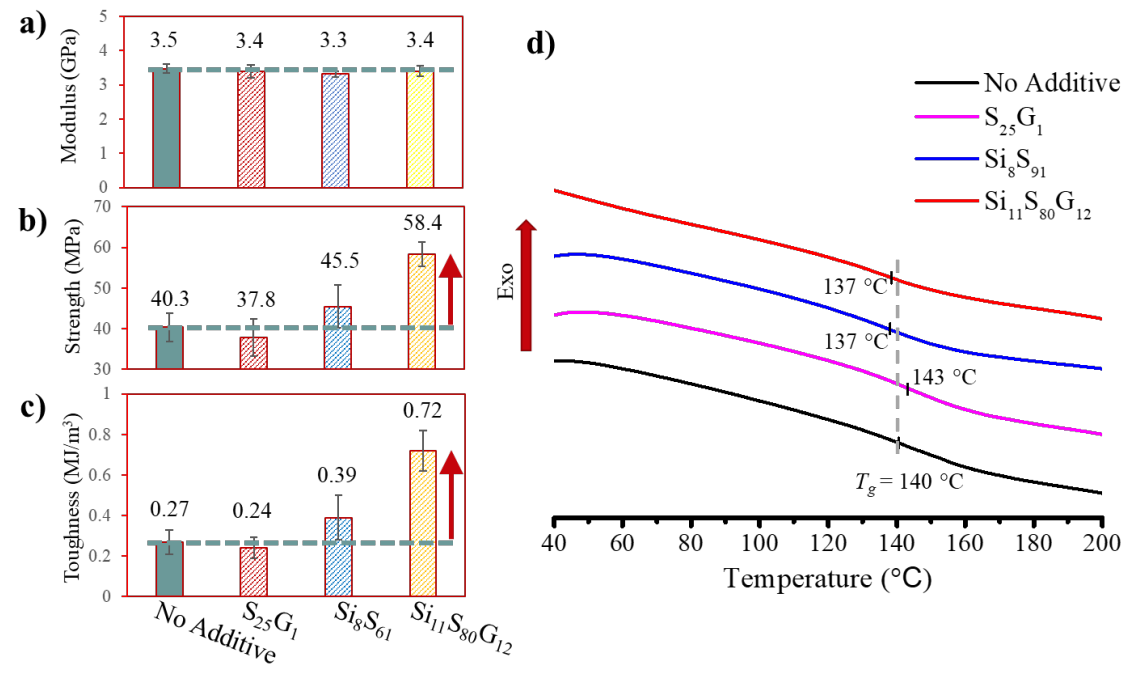


Figure 5: The BCP(1 wt%)/ECC blend was photocrosslinked in a mold to form dog-bone samples and the a) modulus b) failure strength and c) toughness was measured as a function of the composition of the BCP. The arrows indicate the increase of toughness and strength for BCP/ECC blends. d) DSC curves of the cured samples show  $T_g$  (dotted line) comparable for all 4 samples tested.

To understand the toughening mechanism of the BCP additive, we examined the fracture surface of the tensile tested samples by scanning electron microscopy (SEM) (**Figure 6**). The pure ECC fracture surface was a smooth, mostly featureless surface that is characteristic of a brittle failure with low intrinsic toughness. In contrast, the fracture surface of the ECC with BCP additive (Si<sub>11</sub>S<sub>149</sub>G<sub>5</sub>) show a large number of smooth spherical structures of variable sizes uniformly distributed within the matrix, that are fused with the base resin. The spherical aggregates are most likely composed of the BCP bonded to the resin, and the presence of the cracks also agrees with similar observations of crack arrest and deflection in DGEBA/non-reactive triblock copolymer blends [31]. While some of such features are also present in the control blends of ECC/Si<sub>8</sub>S<sub>61</sub>, their shape is more spherical in appearance. The lower toughness in the ECC/Si<sub>8</sub>S<sub>61</sub> blend is attributable to the reduced interfacial adhesion from the lack of covalent bonding leading to lower stress transfer. The fracture surface of ECC/S<sub>25</sub>G<sub>1</sub> is similar to pure ECC resin, as it consists of epoxyphilic PS and PGMA. Hence the presence of elastomeric PMAPDMS is essential for the formation of the spherical aggregates and the resulting intrinsic toughening of the material as the crack develops and progresses.

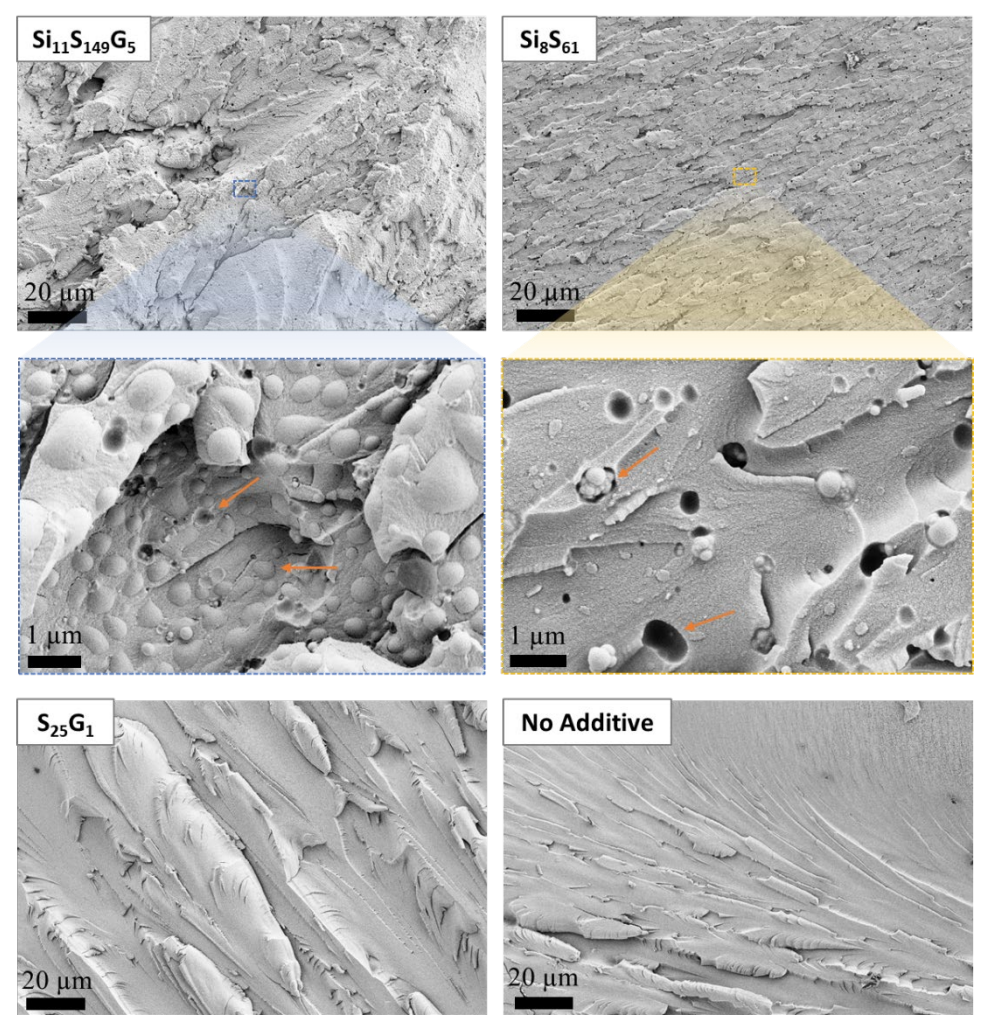


Figure 6: Top-Down SEM images of the fracture surfaces for BCP/ECC blends with insets showing zoom-in view. Orange arrows indicate the spherical aggregates formed by BCP.

An increase in the BCP additive Si<sub>11</sub>S<sub>80</sub>G<sub>12</sub> from 1 to 5 to 10 wt% in the base ECC resin resulted in deterioration of toughness, tensile modulus as well as the tensile strength (**Figure 7**). The optical transparency of the samples also deteriorates leading to opaque cured samples at 10 wt% BCP concentration (Figure 7(a)). The loss of optical transparency indicates the presence of much larger aggregates in the crosslinked blend [32,33]. These larger aggregates serve as macroscale defects leading to the loss of mechanical properties and premature failure. The T<sub>g</sub> measured by DSC shows an increase of 11 °C for the 10 wt% BCP concentration (**Figure S9**). One possible explanation for this increase is due to the increased crosslink density in the cured resin. It should be noted that tensile strength and toughness of the 5 wt% concentration sample are still higher than the base ECC resin though lower than the 1 wt% concentration samples.

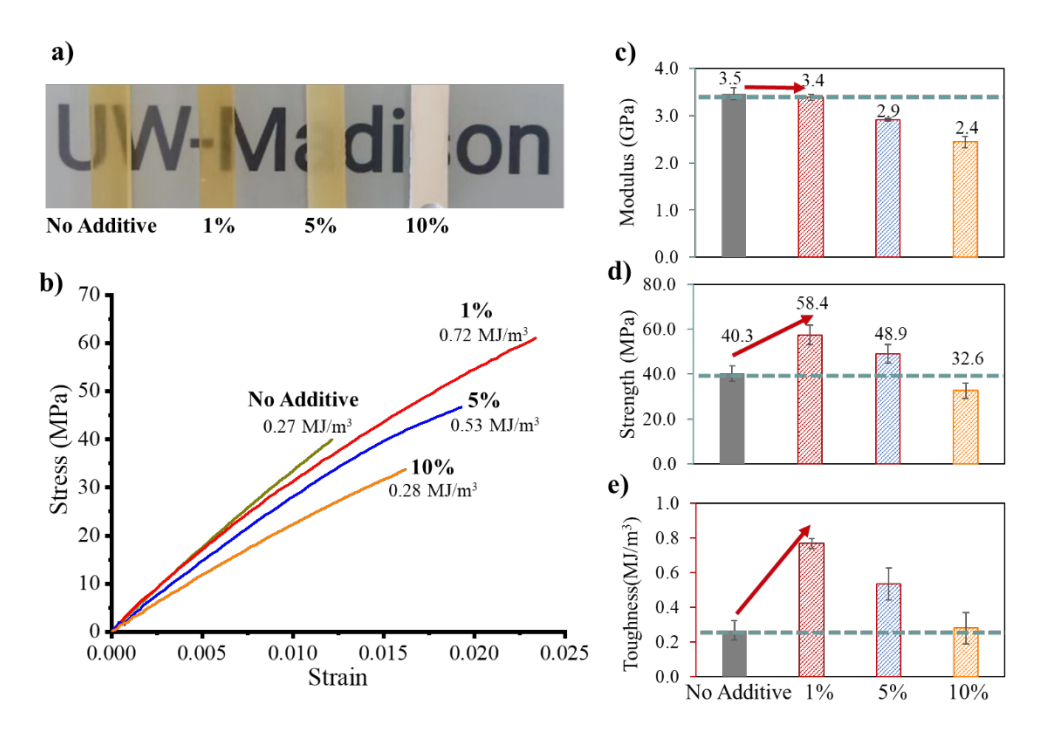


Figure 7: Increased concentration of  $Si_{11}S_{80}G_{12}$  additive to ECC affects the a) optical transparency, b) stress-strain-stress response, c) modulus, d) strength, and e) toughness of the cured blends.

Analysis of the fracture surface of the tensile tested samples using SEM and white light interferometry (Figure 8) show a more complex out-of-plane fracture topography (see the height profile measured normal to the fractured surface in Figure 8(b)) with increase in density of micro fissures and number of aggregates (Figure 8(c)) with increased concentration of Si<sub>11</sub>S<sub>80</sub>G<sub>12</sub> in ECC. The smooth spherical aggregates in the 1 wt% blends (Figure 8(c)) most likely consist of PMAPDMS core with PS and PGMA blocks extending into the ECC resin (Figure 1). The PGMA block by design crosslinks with the epoxy groups in ECC leading to a gradient in crosslinking from low to high as we go into the bulk crosslinked ECC resin. The point at which these aggregates detach from the bulk ECC during tensile testing likely represents the transition into more brittle ECC resin. Upon closer inspection of, for example 5 wt% concentration sample (Figure 8(c)), a large number of craters in addition to spherical aggregates can be observed, which is quite distinct from the 1 wt% sample. As the number of nucleation sites for the formation of these aggregates increases with the increasing concentration of the BCP additive, there exists a tradeoff where the modulus is no longer preserved but the toughness is still higher than the base resin. At the highest concentration of 10 wt% we no longer observe a continuous matrix but more flake-like features, and numerous microcracks, which correlates with the increased T<sub>g</sub>, due to more crosslinks discussed above. In contrast for the pristine samples (before tensile testing) prepared by microtome (Figure S10), no micro-fissures were observed but the spherical aggregates are seen, confirming that the micro-fissures only form during loading and lead to larger cracks, and eventual brittle failure.

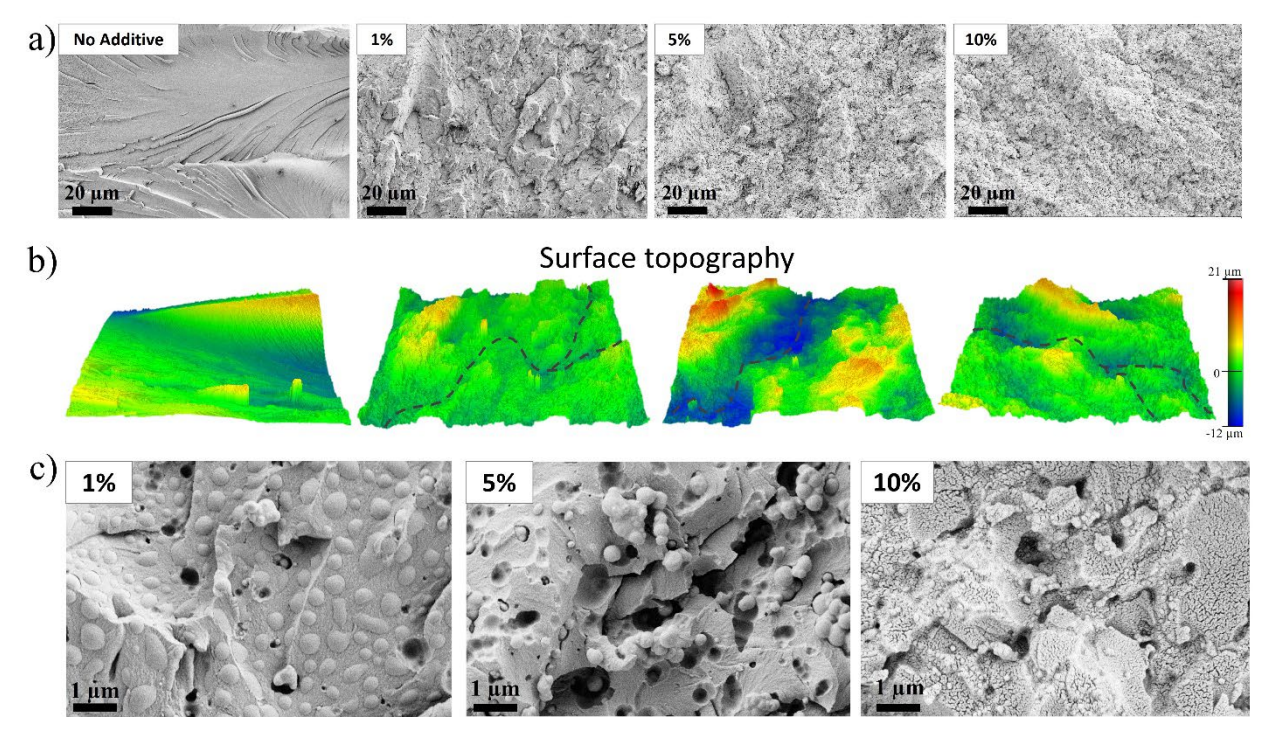


Figure 8: Fracture surface of samples with increasing BCP additive of 0-10 wt% by a) top-down SEM images of the and b) optical profilometer shows roughness of the surface, with the dashed line indicating the possible crack propagation path across the fracture surface. Zoom-in view c) on the fracture surface BCP/ECC blend shows spherical aggregates and microfissures.

We also studied the effect of select changes in the composition of the brush-coil BCP by mainly increasing the polystyrene block length from 24 to 149 repeat units. In fact, the toughness of all the resulting cured blends is 1.3 to 2 times higher than that of the base ECC resin (Figure 9(a), (b)). Increase in the toughness with increase in the PS block length may be attributed to the increased phase segregation tendencies. The  $T_g$  of the crosslinked blends (Figure 9(c)) stays constant at ~ 140 °C and does not change with the PS length.

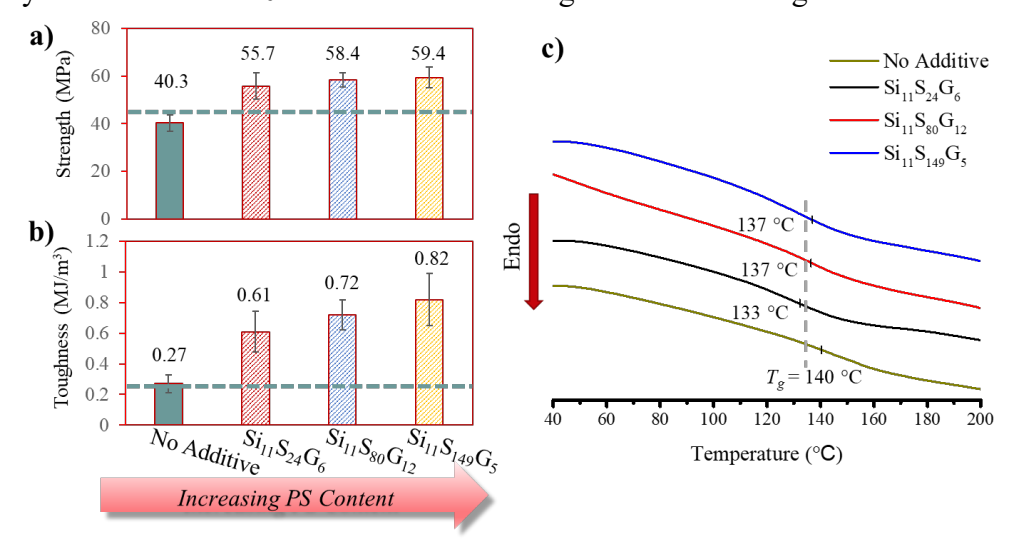


Figure 9: Effect of increasing in the PS block length in the brush-coil BCP additive (1 wt%) in ECC resin was studied for changes to a) Tensile strength, b) Toughness, and c)  $T_g$  by DSC.

## 2.3. DIW printing of ECC resin containing brush-coil BCP Additive

We chose direct ink write (DIW) to demonstrate the printability of the ECC blends. DIW of epoxy resins is quite challenging due to the slow curing kinetics and Newtonian rheological properties [34]. To overcome these issues, chemical modification either through forming hybrid resins (i.e. acrylate-epoxy) [35], added rheological modifiers [36], or a combination of both [37–39] have been explored. Only 2D printing is known for epoxy resin without such additives [40]. Our approach is to lightly precure the resin to create a DIW ink with ideal rheological properties, without any additional additives, which is beneficial for scalability, processing and cost. The pure epoxy resin was thermally precured at 120 °C for increasing amounts of time and the rheological properties characterized (**Figure 10(a)**). When precured for 20 minutes the viscosity increases to 9 Pa·s compared to 0.4 Pa·s for as received ECC. However, the behavior remains Newtonian. After 22 minutes of precuring the prepolymer viscosity increases to 65 Pa·s and exhibits the desired shear thinning behavior for DIW printing. Precuring for longer than 25 minutes resulted in a prepolymer that was too viscous to extrude from an 18-gauge needle used in our custom DIW printer.

Typically, shape fidelity can be achieved with yield stress fluids (they become solid like with the absence of shear) or an external stimulus can be used (such as photocuring). We chose the latter to preserve the shape. DIW printing was performed using a UV-assisted printing setup whereby layers were extruded onto a build platform, photocured to prevent further deformation, and followed by the extrusion of the next layer onto the previously cured layer (Figure 10(b), Figure S11). This approach allows for slight under curing enabling further covalent bonding to form between layers creating good layer adhesion. With this process, we were able to print simple multi- layered objects with well-controlled layer height (Figure 10(c), Table S1). Next, we explore if the toughness still increases in the test samples prepared via DIW printing. Two inks were prepared either containing precured pure ECC or pre- cured ECC/BCP (1 wt% Si<sub>11</sub>S<sub>80</sub>G<sub>12</sub>) blend. After conducting a tensile test (Figure 10(d)), we observed that the 3D printed pure ECC resin sample exhibited comparable mechanical performance to the mold-cast sample. The modulus, failure strength, and toughness were almost identical, indicating that our established 3D printing protocol did not negatively impact the cured ECC resin's performance. With the BCP additive in ECC, as expected higher toughness (0.52 MJ/m<sup>3</sup>), and tensile strength (50.7 MPa), compared to pure ECC (toughness: 0.36 MJ/m<sup>3</sup>, tensile strength: 45.9 MPa), was observed. However, unlike the cast samples the DIW samples showed a decrease in modulus from 3.4 MPa (for pure ECC) to 2.7 MPa with 1 wt% additive. The fracture surface examined with SEM shows the emergence of a complex topography in BCP added sample (Figure 10(e)) compared to the controlled ECC resin, similar to the intrinsic toughening mechanisms seen in the mold-cast samples (Figure 8).

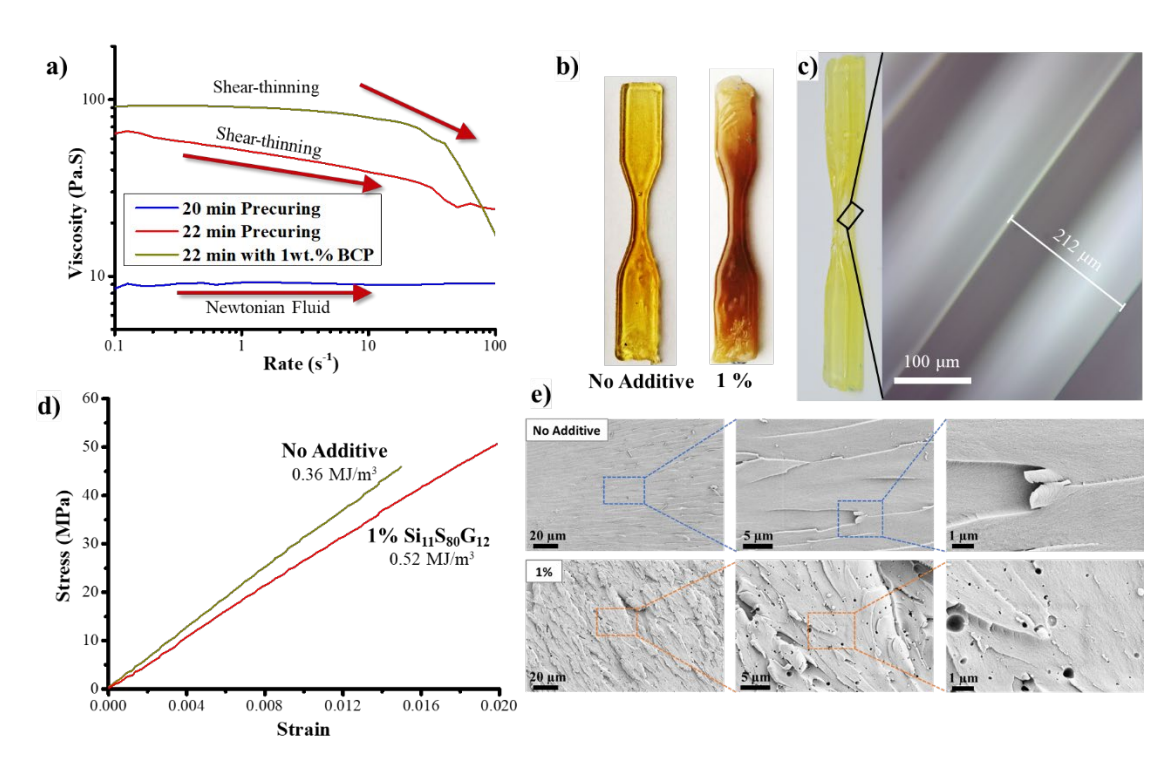


Figure 10: a) ECC resin and its blends with the BCP (1 wt%) were studied for changes to viscosity as a function of shear rate, which clearly show the desired shear thinning behavior of precured prepolymer. b) DIW printed dog bone samples for the ECC and ECC/BCP blends (b) are shown, along with the c) optical microscopy side view image of the samples showing each printed layer line and the layer thickness. d) The stress-strain responses of the printed tensile bars, along with the fracture surface SEM image e).

These results are encouraging as these are to the best of our knowledge, the first examples of DIW of chemically unmodified ECC resin with BCP additives. The reduction in modulus from the cast to the DIW printed samples highlights the challenges of translating bulk properties into printed parts for thermosets such as ECC. These differences we believe are attributable to the precuring processes necessary for the DIW process which may alter the overall miscibility of the BCP additive with the base resin. The photocuring process used in the mold cast samples is very rapid (< 3min), whereas the thermal precuring process is over a larger time frame of ~22 min. These differences in the cure kinetics may also play a role in the miscibility of the BCP additive in the base resin. Further optimization of the precuring process/composition of the BCP additive may be necessary to preserve the modulus of the DIW samples.

## 2.4. DLP printing of ECC/Acrylate mixed resin with BCP additive:

With the success from DIW printing, we examined the use of brush-coil BCP additive in digital light processing (DLP). DLP is a 3D printing technique that utilizes the fast curing of resin by patterned light to achieve the desired shape. Its fast printing speed, good scalability and mild working condition [6], are all highly desirable. One drawback of DLP is the limited available resin chemistries. This is partially a result of the fast (~10 s) photocuring kinetics required for the printing process[41]. This limits the performance of the printed part. In order to expand the application scope of the DLP printing, various approaches have been taken, including the development of new chemistries/photopolymers introducing desired properties [42,43], new

processing techniques [44] and additives [41]. Among them, additives stand out as requiring least modification to the existing DLP technology. BCPs are one of the promising candidates for the toughening of printed objects. To test the application of our brush-coil BCP's in DLP printing, we demonstrated the printing of a mixed ECC/isobornyl acrylate (IBOA) resin with BCP additive.

We chose to use an ECC/IBOA 60:40 wt./wt. mixed resin because the pure ECC cures relatively slowly under UV light (~3 min required [45]) and does not meet the requirements for DLP printing. ECC/IBOA mixed resin, on the other hand, solidifies under 30 s and is known to print using the DLP technique [30,46–48]. We printed the resin using a commercial DLP printer that cures the acrylate monomers with 405 nm UV light to form soft acrylate matrix highly swollen in ECC monomer. When postcured with 365 nm UV light, the remaining ECC completely cures to form an interpenetrating acrylate epoxy network that transforms the part into a rigid material (Figure S12). This process gives well defined shape (Figure 11(b), Figure S13). Using this process, we printed dog bone samples and performed tensile tests to explore whether there is an improvement in the mechanical performance of the BCP blends (Figure 11(c)-(e)). When compared with the resin without additive, cured BCP blends show comparable modulus, yet the failure strength and toughness both increased. A 16% increase in failure strength and 50% increase in toughness is observed. The fracture topography (Figure 11(f)) interestingly is much more complex for both control and BCP samples than what is observed in DIW printed samples (Figure 10). In fact, the interpenetrating network is clearly visible in the SEM with the smoother surface from ECC intermixed with domains of rougher acrylate resin. The specific effect of BCP additive in DIW is not discernable in the SEM images of the fracture surface, however, is evident in the improved mechanical properties (Figure 11(d)-(e)). The PGMA and PS block of the BCP are compatible with both the ECC and the acrylate resins, hence the BCP domains can form aggregates in both acrylate and epoxy domains. It is also likely that the BCP may be acting as a compatibilizer between the acrylate and the epoxy domains leading to improved toughness.

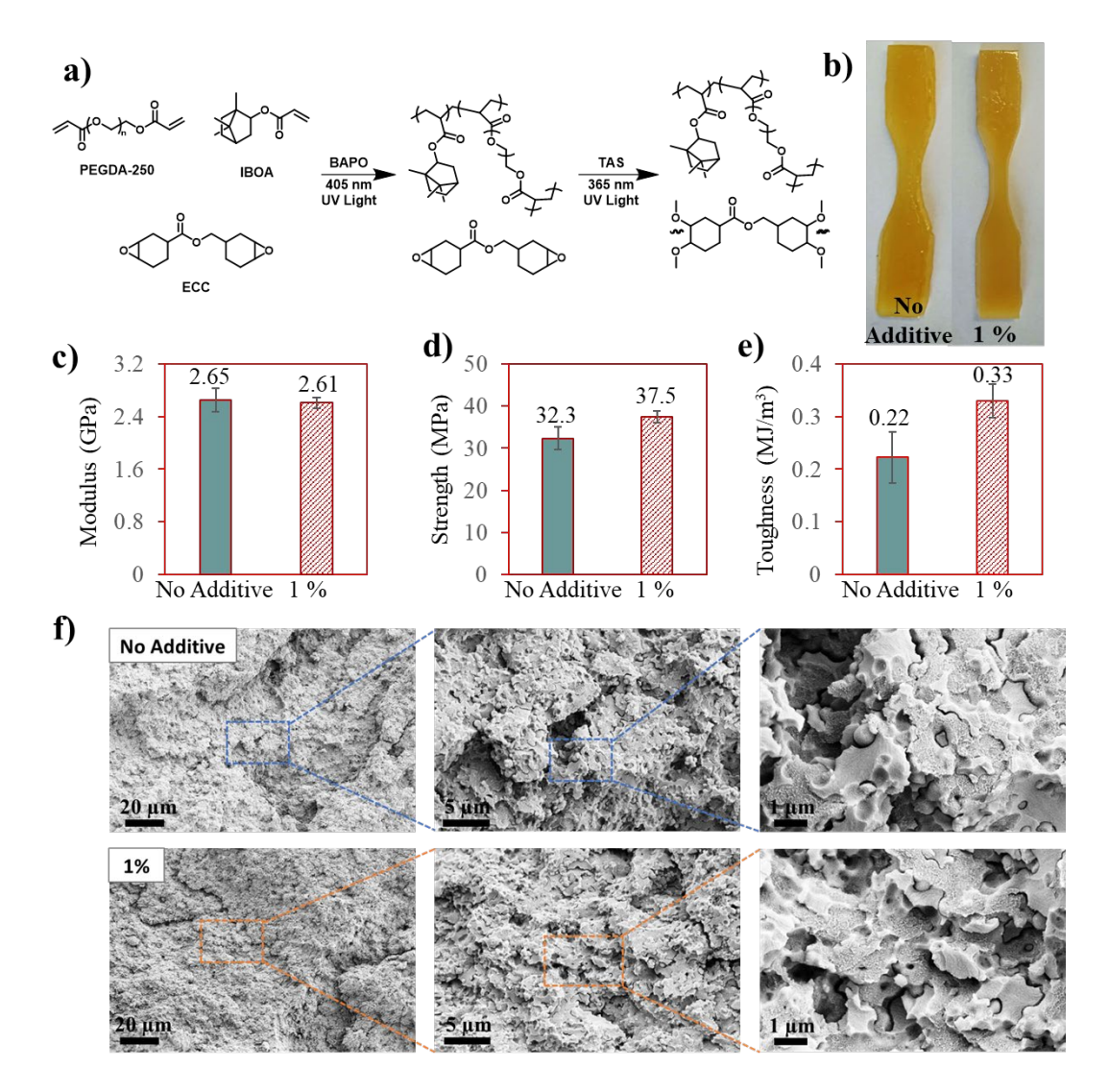


Figure 11: ECC/IBOA 60:40 wt./wt. mixed resin and its blends with the BCP (1 wt%) were studied for a) DLP printing based on the fasting curing kinetic of IBOA and subsequent curing of ECC resin. (b) DLP printed dog bone samples of the ECC/IBOA mixed resin and its blend with BCP (b) are shown, along with the (c) modulus, (d) failure strength and (e) toughness of the cured samples (p value is 0.033). Fracture surface after tensile testing for blends with or without BCP additive were imaged by SEM (f).

## 3. Conclusions

In summary, BCP poly(MAPDMS-b-S-b-GMA) with a brush-coil architecture has been studied as an additive for the toughening of 3D printable cycloaliphatic epoxy resin. The brush-coil architecture was chosen to impart favorable rheological properties and enhanced phase separation characteristics over their linear counterparts. In cast samples that are rapidly photocured, the toughness of ECC improved 2× with only 1 wt% of BCP additive. Analysis of the tested samples indicates that aggregation induced by the BCP additive leads to intrinsic toughening mechanisms, including microfissure formation and crack arrest and deflection, which may explain the observed synergistic strengthening and toughening. This BCP additive was also compatible with 3D printing process. The BCP/ECC blends as well as PCP-ECC/Acrylate

blends were successfully printed using DIW and DLP respectively, and showed improved toughness and strength compared to the base resin. The use of only 1 wt% brush-coil BCP additive compared to the >10 wt% typically required for linear BCPs, minimizes changes in the viscosity of the resin and therefore enhances the compatibility of this additive with the 3D printing process, by keeping the formulation simple and cost effective. This study offers a route to incorporate reactive BCPs to a 3D printable thermosetting resin. Careful attention to the cure kinetics, and the induced morphological changes are critical to simultaneously enhance the toughness without compromising on the modulus.

## **Acknowledgements**

P.G and R.C acknowledge partial support from NSF-DMR-2003891 for the synthesis of the block copolymers and the University of Wisconsin - Madison Office of the Vice Chancellor for Research and Graduate Education with funding from the Wisconsin Alumni Research Foundation for developing the 3D printable resins and their characterization. J.C and R.T acknowledge the partial support from the U. S. Office of Naval Research under PANTHER award number N000142112916 through Dr. Timothy Bentley. We gratefully acknowledge support from the staff and use of the facilities and instrumentation supported by the NSF through the University of Wisconsin Materials Research Science and Engineering Center (DMR-1720415). The Bruker AVANCE 400 NMR spectrometer was supported by the NSF grant CHE-1048642. K.C.H.C acknowledges support from the National Science Foundation Graduate Research Fellowship under Grant No. DGE-1747503. Any opinion, findings, and conclusions or recommendations expressed in this material are those of the authors(s) and do not necessarily reflect the views of the National Science Foundation.

‡ R.C and J.C contributed equally to this work.

#### References

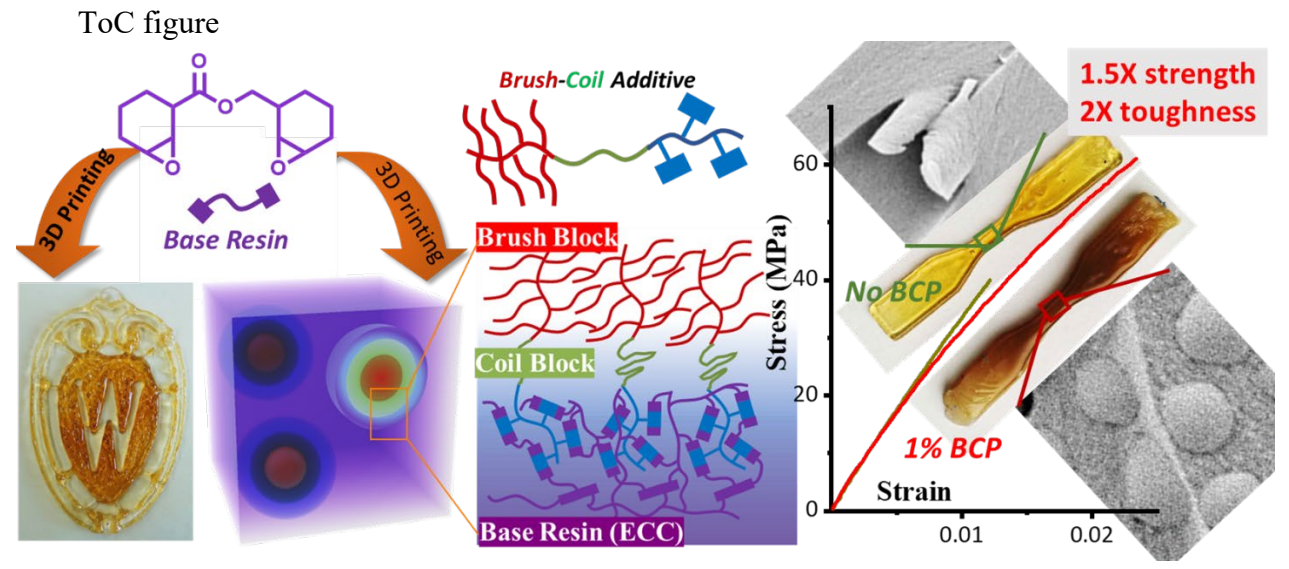
- [1] N.W. Bartlett, M.T. Tolley, J.T.B. Overvelde, J.C. Weaver, B. Mosadegh, K. Bertoldi, G.M. Whitesides, R.J. Wood, A 3D-printed, functionally graded soft robot powered by combustion, Science (80-.). 349 (2015) 161–165. https://doi.org/10.1126/science.aab0129.
- [2] M. Wehner, R.L. Truby, D.J. Fitzgerald, B. Mosadegh, G.M. Whitesides, J.A. Lewis, R.J. Wood, An integrated design and fabrication strategy for entirely soft, autonomous robots, Nature. 536 (2016) 451–455. https://doi.org/10.1038/nature19100.
- [3] A.K. Au, W. Huynh, L.F. Horowitz, A. Folch, 3D-Printed Microfluidics, Angew. Chemie Int. Ed. 55 (2016) 3862–3881. https://doi.org/10.1002/anie.201504382.
- [4] F.P.W. Melchels, M.A.N. Domingos, T.J. Klein, J. Malda, P.J. Bartolo, D.W. Hutmacher, Additive manufacturing of tissues and organs, Prog. Polym. Sci. 37 (2012) 1079–1104. https://doi.org/10.1016/j.progpolymsci.2011.11.007.
- [5] A.J. Boydston, B. Cao, A. Nelson, R.J. Ono, A. Saha, J.J. Schwartz, C.J. Thrasher, Additive manufacturing with stimuli-responsive materials, J. Mater. Chem. A. 6 (2018) 20621–20645. https://doi.org/10.1039/C8TA07716A.
- [6] Z. Zhao, X. Tian, X. Song, Engineering materials with light: Recent progress in digital light processing based 3D printing, J. Mater. Chem. C. 8 (2020) 13896–13917. https://doi.org/10.1039/d0tc03548c.
- [7] M.A.S.R. Saadi, A. Maguire, N.T. Pottackal, M.S.H. Thakur, M.M. Ikram, A.J. Hart, P.M. Ajayan, M.M. Rahman, Direct Ink Writing: A 3D Printing Technology for Diverse Materials, Adv. Mater. 34 (2022) 1–57. https://doi.org/10.1002/adma.202108855.
- [8] A.C. Garg, Y.W. Mai, Failure mechanisms in toughened epoxy resins-A review, Compos. Sci. Technol. 31

- (1988) 179-223. https://doi.org/10.1016/0266-3538(88)90009-7.
- [9] R. Bagheri, B.T. Marouf, R.A. Pearson, Rubber-toughened epoxies: A critical review, Polym. Rev. 49 (2009) 201–225. https://doi.org/10.1080/15583720903048227.
- [10] L. Ruiz-Pérez, G.J. Royston, J.P.A. Fairclough, A.J. Ryan, Toughening by nanostructure, Polymer (Guildf). 49 (2008) 4475–4488. https://doi.org/10.1016/j.polymer.2008.07.048.
- [11] D.A. Norman, R.E. Robertson, Rigid-particle toughening of glassy polymers, Polymer (Guildf). 44 (2003) 2351–2362. https://doi.org/10.1016/S0032-3861(03)00084-3.
- [12] Q. Guo, J.M. Dean, R.B. Grubbs, F.S. Bates, Block copolymer modified novolac epoxy resin, J. Polym. Sci. Part B Polym. Phys. 41 (2003) 1994–2003. https://doi.org/10.1002/polb.10554.
- [13] R.B. Grubbs, J.M. Dean, M.E. Broz, F.S. Bates, Reactive block copolymers for modification of thermosetting epoxy, Macromolecules. 33 (2000) 9522–9534. https://doi.org/10.1021/ma001414f.
- [14] S. Ritzenthaler, F. Court, E. Girard-Reydet, L. Leibler, J.P. Pascault, ABC triblock copolymers/epoxy-diamine blends. 2. Parameters controlling the morphologies and properties, Macromolecules. 36 (2003) 118–126. https://doi.org/10.1021/ma0211075.
- [15] L. Tao, Z. Sun, W. Min, H. Ou, L. Qi, M. Yu, Improving the toughness of thermosetting epoxy resins: Via blending triblock copolymers, RSC Adv. 10 (2020) 1603–1612. https://doi.org/10.1039/c9ra09183a.
- [16] F. Nian, J. Ou, Q. Yong, Y. Zhao, H. Pang, B. Liao, Reactive block copolymers for the toughening of epoxies: Effect of nanostructured morphology and reactivity, J. Macromol. Sci. Part A Pure Appl. Chem. 55 (2018) 533–543. https://doi.org/10.1080/10601325.2018.1476826.
- [17] J. Moon, Y. Huh, S. Kim, Y. Choe, J. Bang, Reactive Core-Shell Bottlebrush Copolymer as Highly Effective Additive for Epoxy Toughening, Chinese J. Polym. Sci. 39 (2021) 1626–1633. https://doi.org/10.1007/s10118-021-2614-z.
- [18] L.C. Jheng, I.H. Wang, T.H. Hsieh, C.T. Fan, C.H. Hsiao, C.P. Wu, M.T. Leu, T.Y. Chang, Toughening of epoxy thermosets with nano-sized or micron-sized domains of poly(ethylene oxide)-b-poly(butadiene-co-acrylonitrile)-b-poly(ethylene oxide) triblock copolymers synthesized using room temperature ester coupling reaction, J. Appl. Polym. Sci. 138 (2021) 1–12. https://doi.org/10.1002/app.50096.
- [19] H.M. Chong, A.C. Taylor, The microstructure and fracture performance of styrene-butadiene-methylmethacrylate block copolymer-modified epoxy polymers, J. Mater. Sci. 48 (2013) 6762–6777. https://doi.org/10.1007/s10853-013-7481-8.
- [20] B. Narupai, A. Nelson, 100th Anniversary of Macromolecular Science Viewpoint: Macromolecular Materials for Additive Manufacturing, ACS Macro Lett. 9 (2020) 627–638. https://doi.org/10.1021/acsmacrolett.0c00200.
- [21] R. d'Arcy, J. Burke, N. Tirelli, Branched polyesters: Preparative strategies and applications, Adv. Drug Deliv. Rev. 107 (2016) 60–81. https://doi.org/10.1016/j.addr.2016.05.005.
- [22] Z. Li, M. Tang, S. Liang, M. Zhang, G.M. Biesold, Y. He, S.M. Hao, W. Choi, Y. Liu, J. Peng, Z. Lin, Bottlebrush polymers: From controlled synthesis, self-assembly, properties to applications, Prog. Polym. Sci. 116 (2021) 101387. https://doi.org/10.1016/j.progpolymsci.2021.101387.
- [23] G. Xie, M.R. Martinez, M. Olszewski, S.S. Sheiko, K. Matyjaszewski, Molecular Bottlebrushes as Novel Materials, Biomacromolecules. 20 (2019) 27–54. https://doi.org/10.1021/acs.biomac.8b01171.
- [24] J. Huang, A. Hall, I. Jayapurna, S. Algharbi, V. Ginzburg, T. Xu, Nanocomposites Based on Coil-Comb Diblock Copolymers, Macromolecules. (2021). https://doi.org/10.1021/acs.macromol.0c02441.
- [25] J. Rzayev, Molecular bottlebrushes: New opportunities in nanomaterials fabrication, ACS Macro Lett. 1 (2012) 1146–1149. https://doi.org/10.1021/mz300402x.
- [26] D. Neugebauer, Y. Zhang, T. Pakula, K. Matyjaszewski, PDMS-PEO densely grafted copolymers, Macromolecules. 38 (2005) 8687–8693. https://doi.org/10.1021/ma0514828.
- [27] J. Rieger, The glass transition temperature of polystyrene, J. Therm. Anal. 46 (1996) 965–972. https://doi.org/10.1007/bf01983614.
- [28] W. Fan, L. Wang, S. Zheng, Nanostructures in thermosetting blends of epoxy resin with polydimethylsiloxane-block-poly(ε-caprolactone)-block-polystyrene ABC triblock copolymer, Macromolecules. 42 (2009) 327–336. https://doi.org/10.1021/ma8018014.
- [29] I. Tzoumani, A. Soto Beobide, Z. Iatridi, G.A. Voyiatzis, G. Bokias, J.K. Kallitsis, Glycidyl Methacrylate-Based Copolymers as Healing Agents of Waterborne Polyurethanes, Int. J. Mol. Sci. 23 (2022).

- https://doi.org/10.3390/ijms23158118.
- [30] J.J. Schwartz, A.J. Boydston, Multimaterial actinic spatial control 3D and 4D printing, Nat. Commun. 10 (2019) 1–10. https://doi.org/10.1038/s41467-019-08639-7.
- [31] J. Liu, H.J. Sue, Z.J. Thompson, F.S. Bates, M. Dettloff, G. Jacob, N. Verghese, H. Pham, Nanocavitation in self-assembled amphiphilic block copolymer-modified epoxy, Macromolecules. 41 (2008) 7616–7624. https://doi.org/10.1021/ma801037q.
- [32] D. Carolan, A. Ivankovic, A.J. Kinloch, S. Sprenger, A.C. Taylor, Toughening of epoxy-based hybrid nanocomposites, Polymer (Guildf). 97 (2016) 179–190. https://doi.org/10.1016/j.polymer.2016.05.007.
- [33] Q.H. Le, H.C. Kuan, J. Bin Dai, I. Zaman, L. Luong, J. Ma, Structure-property relations of 55nm particle-toughened epoxy, Polymer (Guildf). 51 (2010) 4867–4879. https://doi.org/10.1016/j.polymer.2010.08.038.
- [34] K.B. Manning, N. Wyatt, L. Hughes, A. Cook, N.H. Giron, E. Martinez, C.G. Campbell, M.C. Celina, Self Assembly–Assisted Additive Manufacturing: Direct Ink Write 3D Printing of Epoxy–Amine Thermosets, Macromol. Mater. Eng. 304 (2019) 1–16. https://doi.org/10.1002/mame.201800511.
- [35] K. Chen, X. Kuang, V. Li, G. Kang, H.J. Qi, Fabrication of tough epoxy with shape memory effects by UV-assisted direct-ink write printing, Soft Matter. 14 (2018) 1879–1886. https://doi.org/10.1039/c7sm02362f.
- [36] B.G. Compton, J.A. Lewis, 3D-printing of lightweight cellular composites, Adv. Mater. 26 (2014) 5930–5935. https://doi.org/10.1002/adma.201401804.
- [37] M. Invernizzi, G. Natale, M. Levi, S. Turri, G. Griffini, UV-assisted 3D printing of glass and carbon fiber-reinforced dual-cure polymer composites, Materials (Basel). 9 (2016). https://doi.org/10.3390/MA9070583.
- [38] Q. Shi, K. Yu, X. Kuang, X. Mu, C.K. Dunn, M.L. Dunn, T. Wang, H. Jerry Qi, Recyclable 3D printing of vitrimer epoxy, Mater. Horizons. 4 (2017) 598–607. https://doi.org/10.1039/c7mh00043j.
- [39] C.D. Armstrong, L. Yue, F. Demoly, K. Zhou, H.J. Qi, Unstructured Direct Ink Write 3D Printing of Functional Structures with Ambient Temperature Curing Dual-Network Thermoset Ink, Adv. Intell. Syst. 5 (2023) 2200226. https://doi.org/10.1002/aisy.202200226.
- [40] W. Voit, K. V. Rao, W. Zapka, Direct-write process for UV-curable epoxy materials by inkjet technology, Mater. Res. Soc. Symp. Proc. 758 (2003) 93–99. https://doi.org/10.1557/proc-758-ll3.5.
- [41] A. Medellin, W. Du, G. Miao, J. Zou, Z. Pei, C. Ma, Vat photopolymerization 3d printing of nanocomposites: A literature review, J. Micro Nano-Manufacturing. 7 (2019). https://doi.org/10.1115/1.4044288.
- [42] G.A. Appuhamillage, N. Chartrain, V. Meenakshisundaram, K.D. Feller, C.B. Williams, T.E. Long, 110th Anniversary: Vat Photopolymerization-Based Additive Manufacturing: Current Trends and Future Directions in Materials Design, Ind. Eng. Chem. Res. 58 (2019) 15109–15118. https://doi.org/10.1021/acs.iecr.9b02679.
- [43] C. Choi, Y. Okayama, P.T. Morris, L.L. Robinson, M. Gerst, J.C. Speros, C.J. Hawker, J. Read de Alaniz, C.M. Bates, Digital Light Processing of Dynamic Bottlebrush Materials, Adv. Funct. Mater. 32 (2022). https://doi.org/10.1002/adfm.202200883.
- [44] B. Steyrer, B. Busetti, G. Harakály, R. Liska, J. Stampfl, Hot Lithography vs. room temperature DLP 3D-printing of a dimethacrylate, Addit. Manuf. 21 (2018) 209–214. https://doi.org/10.1016/j.addma.2018.03.013.
- [45] A. Udagawa, Y. Yamamoto, Y. Inoue, R. Chûjô, Physical Properties and Photoreactivity of Cycloaliphatic Epoxy Resins Cured by UV-Induced Cationic Polymerization, Polym. J. 23 (1991) 1081–1090. https://doi.org/10.1295/polymj.23.1081.
- [46] A. Fantoni, J. Ecker, M. Ahmadi, T. Koch, J. Stampfl, R. Liska, S. Baudis, Green Monomers for 3D Printing: Epoxy-Methacrylate Interpenetrating Polymer Networks as a Versatile Alternative for Toughness Enhancement in Additive Manufacturing, ACS Sustain. Chem. Eng. (2023). https://doi.org/10.1021/acssuschemeng.3c02194.
- [47] I. Binyamin, E. Grossman, M. Gorodnitsky, D. Kam, S. Magdassi, 3D Printing Thermally Stable High-Performance Polymers Based on a Dual Curing Mechanism, Adv. Funct. Mater. 33 (2023). https://doi.org/10.1002/adfm.202214368.
- [48] X. Kuang, J. Wu, K. Chen, Z. Zhao, Z. Ding, F. Hu, D. Fang, H.J. Qi, Grayscale digital light processing 3D printing for highly functionally graded materials, Sci. Adv. 5 (2019) 1–10. https://doi.org/10.1126/sciadv.aav5790.

# Block Copolymer Additives for Toughening 3D Printable Epoxy Resin

Ri Chen<sup>a‡</sup>, Jizhe Cai<sup>b‡</sup>, Kyle C. H.Chin<sup>d</sup>, Sheng Wang<sup>a</sup>, A J Boydston<sup>a,c,d</sup>, Ramathasan Thevamaran<sup>b\*</sup>, Padma Gopalan<sup>a,c,d,\*</sup>



A brush-coil block copolymer (BCP) is studied as an additive for the toughening a 3D printable cycloaliphatic epoxy resin. Adding just 1 wt % of the BCP to the epoxy results in a synergistic improvement in strength ( $\sim$ 1.5×) and toughness ( $\sim$ 2×). This additive is compatible with DIW and DLP 3D printing processes and shows similar toughening effect for the printed samples.